Household-level electric vehicle assignment for city-scale agent-based transport simulation

Shuai Zhang*[1], Afshin Jafari[1], Alan Both[1], and Chris De Gruyter[1]

[1]Centre for Urban Research, School of Global, Urban and Social Studies, RMIT University, Australia

Short summary

This study aims to advance the methodological capabilities of agent-based transport simulation models to improve the accuracy of simulated traffic volumes and generate electric vehicle travel demand for further charging studies. It presents an extension to the synthetic population and activity-based demand generation of an existing MATSim model for Greater Melbourne by incorporating a household-level car availability and assignment for both regular vehicles and electric vehicles and for people living in different types of dwelling and household. These contributions are needed because growing electric vehicle adoption and dwelling-type differences drive heterogeneous charging behaviour. Within-household interactions shape individual travel demand and, in turn, electric vehicle energy consumption, both of which are key to charging demand estimates and infrastructure planning. The findings highlight the potential significant benefits in travel demand generation and power grid load prediction using transport models when accounting for the complex mechanisms of household resource constraint, assignment and behaviour.
Keywords: Agent-based modelling, Electric vehicle, Synthetic population, Household car assignment

1 Introduction

Currently, acquiring granular data on electric vehicle (EV) driver behaviour remains a critical challenge for modelling and studying charging demand. While data-driven methods employing machine learning have been widely applied to predict charging demand (Shanmuganathan et al., 2022; Wang et al., 2023; Boulakhbar et al., 2022), these approaches necessitate extensive historical datasets which are often unavailable in early-adoption regions. Consequently, agent-based transport simulations have emerged as another vital method (Guo et al., 2024; Zhang et al., 2023), offering the potential to generate reasonable travel and charging demand patterns using limited survey data.

In agent-based modelling, synthetic population generation has been widely used to represent heterogeneity in household and individual attributes (Weiss & Habib, 2020; Hu et al., 2023; Yang et al., 2025). Nevertheless, a critical methodological oversight persists regarding the incorporation of household attributes and within-household interactions. Although recent studies have noted the influence of household characteristics on mode choice and activity scheduling (Aemmer & MacKenzie, 2022; Khachman et al., 2024; Qiang et al., 2025), frameworks that explicitly model the private car as a finite, shared resource with specific driver–vehicle pairing remain scarce. Neglecting these constraints likely leads to an overestimation of vehicle availability and an inaccurate representation of travel demand. Addressing this gap is critical for the accurate simulation of large-scale EV utilisation given significant impact of travel demand on energy usage. Consequently, the primary objective of this study is to advance the methodological capabilities of agent-based transport simulation by integrating a household-level car assignment model specifically calibrated for generating EV travel demand. Unlike most traditional unconstrained models, our method constructs a household-level population that captures key household and dwelling attributes.

2 Methodology

In this section, we introduce all the datasets used in this paper and the methodology on household-level simulation model. Figure 1 illustrates the overview of datasets, methods(Wickramasinghe et

al., 2020; Both et al., 2021) and steps of this paper. Three datasets were used. (i) the Victorian Integrated Survey of Travel and Activity (VISTA) supplies household attributes including household car count, members, dwelling type, and licence status. (ii) Ausgrid (2023) provides observed marginal distributions of household type and dwelling type among EV-owning households. (iii) the Whole Fleet Vehicle Registration Snapshot by Postcode dataset (Victoria; Q2 2023–Q1 2025) is used to derive postcode-level EV shares.

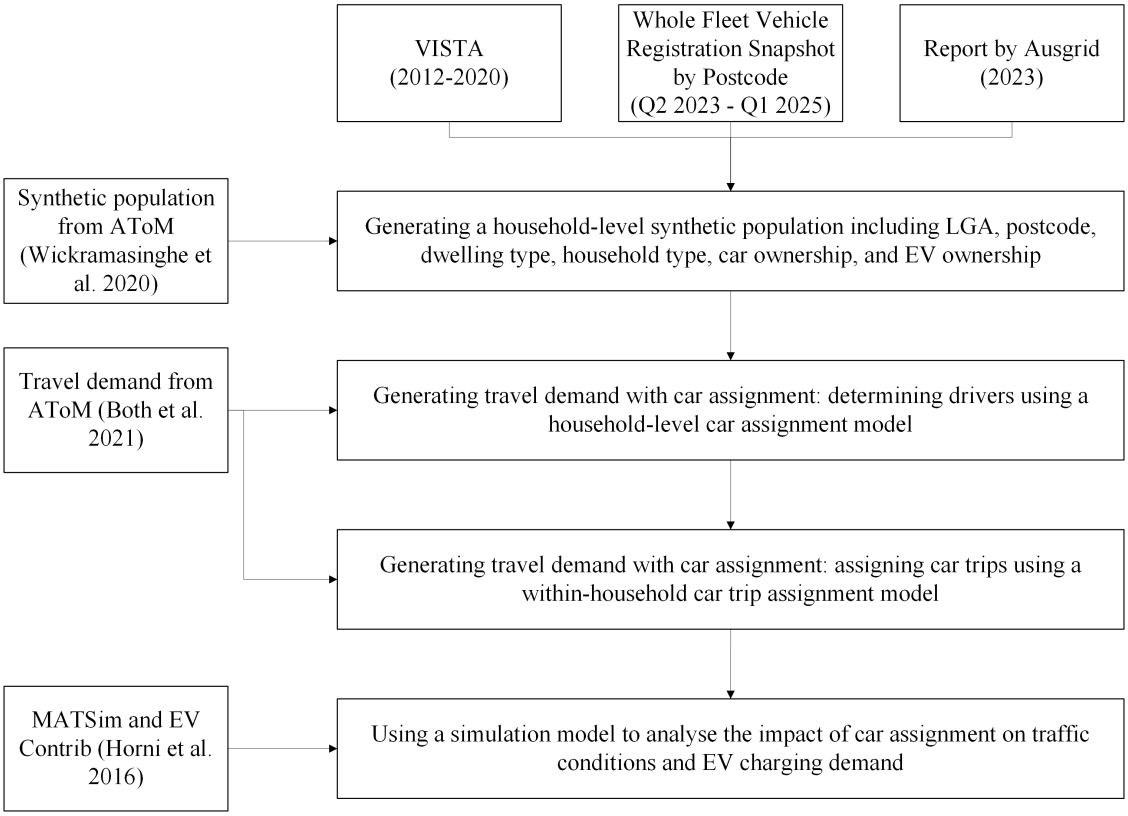


Figure 1: Overview of datasets, methods and steps of this study

Household EV ownership assignment

Let EV be a binary indicator ($EV = 1$ if a household owns an EV). Let H denote household type and D denote dwelling type. Households were grouped into five household types ($ht \in \{1, \ldots, 5\}$) as shown in Table 1 and three dwelling types ($dt \in \{\text{House}, \text{Apartment}, \text{Townhouse}\}$). Let p_{ht} and q_{dt} denote the conditional marginal distribution of household type ht and dwelling type dt among EV-owning households respectively as Equation 1. From Ausgrid (2023), we obtained the conditional marginal distributions among EV-owning households as shown in Table 2 and 3 ($100 \times p_{ht}$ and $100 \times q_{dt}$ as percentages).

$$p_{ht} = P(H = ht \mid EV = 1), \qquad q_{dt} = P(D = dt \mid EV = 1). \tag{1}$$

Table 1: Distribution of household types across the entire sample(164,432 households)

Household type	Adults	Children	Percentage
1	2	≥1	22.0%
2	2	0	33.2%
3	1	≥1	2.9%
4	1	0	22.9%
5	Others		19.0%
Total			100.0%

Table 2: Composition of EV-owning households by household type

Household type	Adults	Children	Percentage
1	2	≥1	50.0%
2	2	0	33.0%
3	1	≥1	2.0%
4	1	0	6.0%
5	Others		9.0%
Total			100.0%

Table 3: Composition of EV-owning households by dwelling type

Dwelling type	Proportion
House	78.0%
Apartment	10.0%
Townhouse	12.0%
Total	100.0%

Because only one-dimensional marginals are available, we reconstructed the joint distribution $P(H = ht, D = dt \mid EV = 1)$ using Iterative Proportional Fitting (IPF) so that the fitted joint distribution was consistent with both marginals.
From the synthetic population we computed the baseline joint distribution of all households using Equation 2.

$$s_{ht,dt} = P(H = ht, D = dt). \tag{2}$$

We then defined a propensity weight as Equation 3.

$$w_{ht,dt} = \frac{P(H = ht, D = dt \mid EV = 1)}{s_{ht,dt}}, \tag{3}$$

This weighting was applied within each postcode so that EV assignments remained consistent with the local household and dwelling-type composition across postcodes, rather than imposing a uniform EV-owner profile citywide.
For each postcode k, the target number of EV-owning households was calculated using Equation 4.

$$N_{EV,k} = \text{round}(\pi_k N_k)\,, \tag{4}$$

where N_k is the total number of households in postcode k and π_k is the postcode-level EV share derived from registration data. Due to data limitations, we assume each EV-owning household owns one EV and treat π_k as the proportion of EV-owning households.
To preserve the area-specific household and dwelling-type composition, we performed EV assignment independently within each postcode. We first construct a three-dimensional grid of cells $\text{cell}(k, ht, dt)$, where each cell contained households located in postcode k with household type ht and dwelling type dt. Let $N_{k,ht,dt}$ denote the number of households in $\text{cell}(k, ht, dt)$.
We assigned $N_{EV,k}$ across cells in proportion to both the local housing stock and the propensity weights $w_{ht,dt}$. The expected number of EV households assigned to each cell is calculated using Equation 5.

$$n_{k,ht,dt} = N_{EV,k}\,\frac{w_{ht,dt}\,N_{k,ht,dt}}{\sum_{ht,dt} w_{ht,dt}\,N_{k,ht,dt}}. \tag{5}$$

Within each $\text{cell}(k, ht, dt)$, $n_{k,ht,dt}$ households were randomly drawn and labelled as $EV = 1$, and all remaining households were labelled as $EV = 0$.

Household-level car assignment and within-household car trip assignment

A 10% sample of households were selected from AToM's synthetic population to preserve household membership. Using the method introduced earlier, we enriched the synthetic population with spatial units, dwelling type, car ownership, EV ownership, and household type.

As shown in Figure 2, we applied a dual-stage framework comprising household-level car assignment and within-household car trip assignment. The framework constrained simultaneous car utilisation so that concurrent usage by household members does not exceed the total number of owned cars, explicitly treating the private car as a finite shared household resource (Figure 3). Household-level car assignment determined real drivers by comparing members' daily travel plans. Three strategies were implemented: Longest-distance-first (LDF), assigning cars in descending order of planned trip distance; First-starting, first-served (FSFS), assigning cars in ascending order of first-trip start time; and Random, assigning cars at random. Within EV-owning households, EVs were prioritised to identify the EV driver and the corresponding EV-specific travel demand.

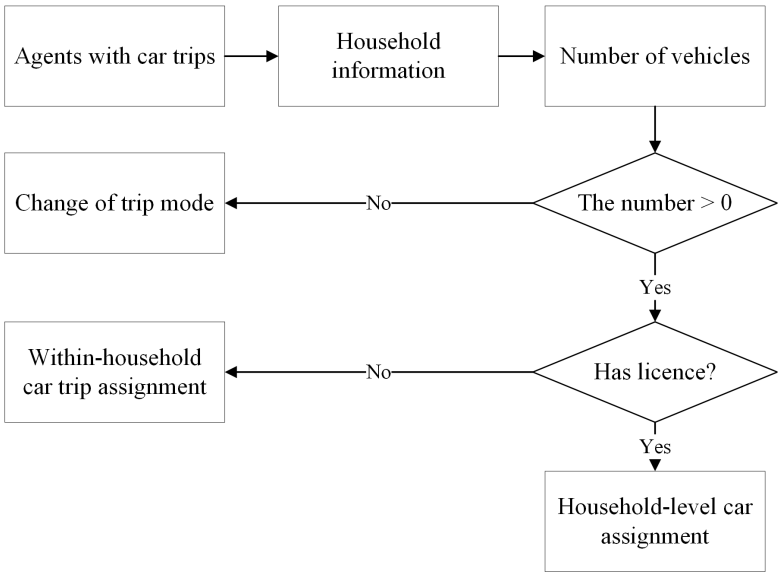


Figure 2: Household car assignment

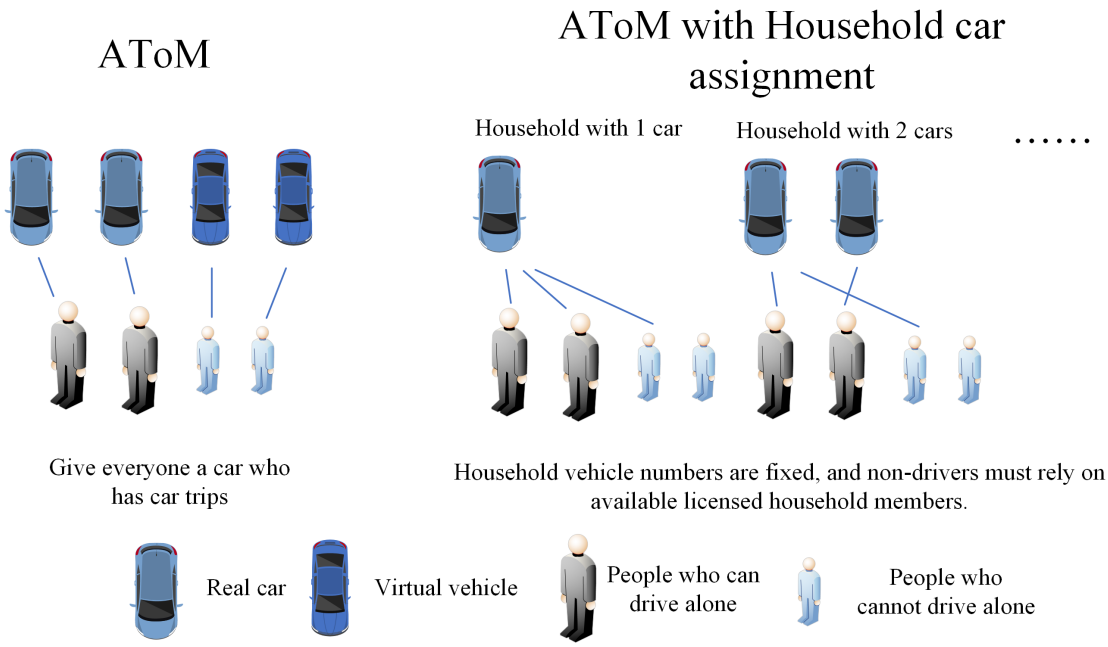


Figure 3: Comparison of the original AToM car assignment and the new household car assignment

For agents with car trips who were identified as unable to drive, their car trips were assigned to other household members who can drive them, where possible. Car trip assignment was restricted to within-household, with the primary objective of minimising the loss of car trips. First, using

the driver's trip as a reference, we assessed temporal assignability. A pair of trips was considered compatible if their overlapping time window exceeds a threshold α:

$$T_{\text{earliest_arr}} - T_{\text{latest_dep}} \geq \alpha \tag{6}$$

where

$$T_{\text{latest_dep}} = \max\left(t^D_{\text{dep}}, t^P_{\text{dep}}\right), \tag{7}$$

$$T_{\text{earliest_arr}} = \min\left(t^D_{\text{arr}}, t^P_{\text{arr}}\right), \tag{8}$$

and $\alpha = 1,800$ seconds (30 minutes). In the VISTA Trips data, the weighted 90th percentile of pick-up/drop-off travel time is 30 minutes, supporting $\alpha = 1800$s.
Second, spatial assignability was assessed by calculating the additional travel distance. Let $d(o_1, o_2)$ be the Euclidean distance between the origins of the two trips, and $d(d_1, d_2)$ be the Euclidean distance between their respective destinations. A trip was considered assignable in terms of distance if the total detour is within a threshold β:

$$d(o_1, o_2) + d(d_1, d_2) \leq \beta \tag{9}$$

where $\beta = 33,000$ m (33 km). In the VISTA Stops data, the weighted 90th percentile of the "go-and-return" access distance (inbound + outbound legs) is around 33km, supporting $\beta = 33$,km and mainly filtering extreme matches.
If new car trips were identified, two new activities "pick-up" and "drop-off" were added to the driver's travel plan as shown in Figure 4. Both "pick-up" and "drop-off" activities were assigned a fixed duration of 30 seconds. If the assignment results in delays to the activities of either drivers or passengers, the trip assignment was rejected.

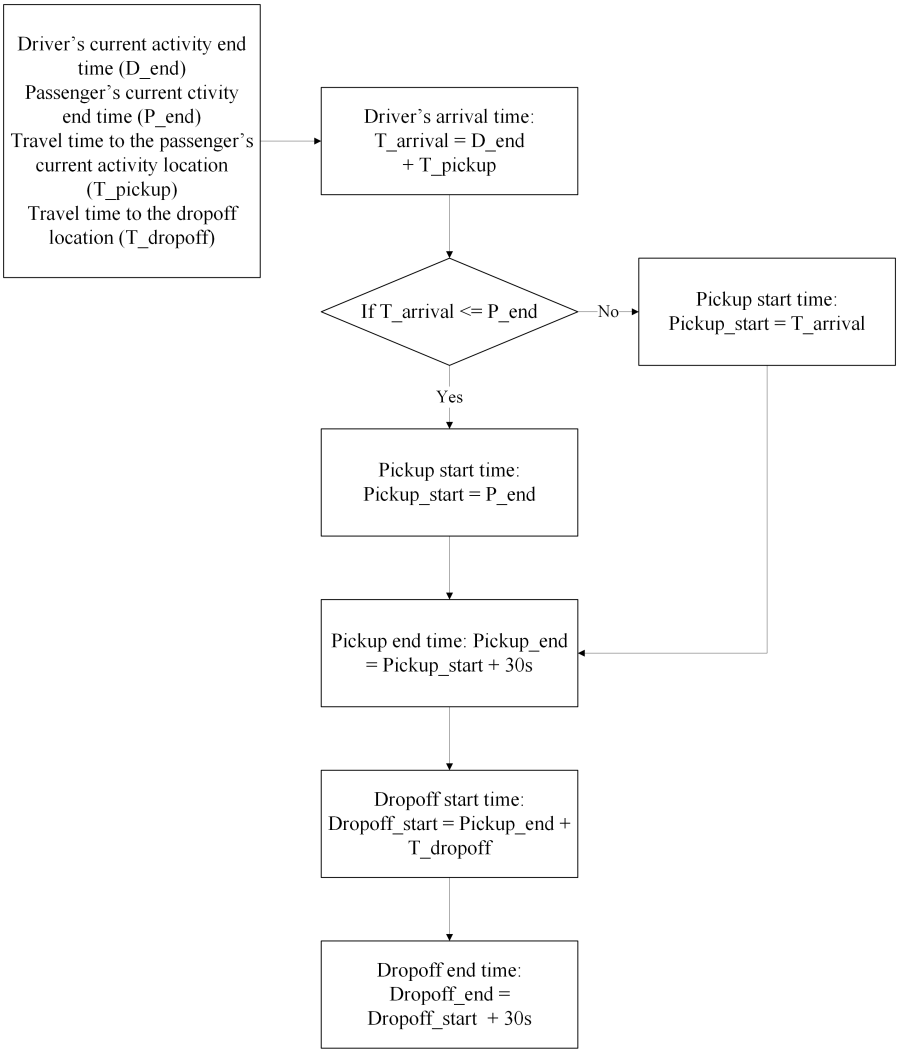


Figure 4: Start and end time settings for the "pick-up" and "drop-off" activities

For households with multiple feasible driver and passenger assignments (i.e., more than one member can serve as the driver), we used a utility function to resolve the final assignment as Equation 10.

$$U_{\text{assign}} = w_t \times \sum T_{\text{waiting}} + w_d \times \sum D_{\text{extra}} + w_n \times N_{\text{trips}} \tag{10}$$

where T_{waiting} is the total waiting time if trips are relocated in the plan, D_{extra} is the extra driving distance if trips are relocated in the plan, and N_{trips} is the number of trips in the new plan. We set $w_t = 0.1$, $w_d = 0.5$, $w_n = 0.4$.
To preserve the integrity of daily activity chains, the model integrated a mode substitution mechanism as a definitive fallback. Specifically, in instances where a trip cannot be accommodated by household vehicle resources, whether through direct car assignment or within-household car trip assignment, the travel mode was automatically converted from "Car" to "Public Transport (PT)".

EV travel demand simulation

Traffic and EV charging demand were simulated using MATSim 2025 with EV Contrib (Horni et al., 2016). Link-flow capacities were scaled by 0.1 to match the 10% household sample. Agents travel by car, public transport, cycling, and walking; parameter settings followed Jafari et al. (2024). Reassigned passenger legs used a dedicated "passenger" teleport mode with zero utility. The only enabled re-planning strategy was "re-routing" (150 iterations; re-planning disabled in the final 30 iterations).
Charging was modelled using EV Contrib "StrategicCharging" for EV drivers only. Public chargers were represented by two power classes (50 kW and 200 kW; as Figure 5), and each EV owner was assigned a 10 kW home charger. Initial state of charge (SoC) was bounded to 20–100% with a 20% charging threshold; the search radius was 10 km; activity charging had a 900 s minimum duration; en-route charging duration was 900–3600 s with a maximum waiting time of 300 s.

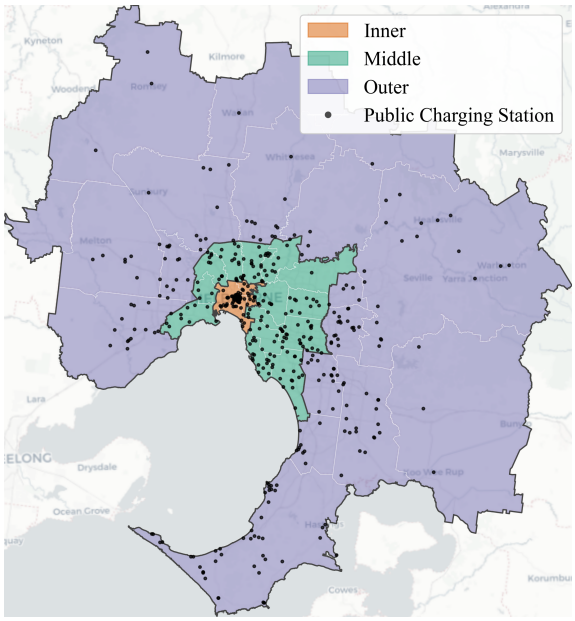


Figure 5: Map of the study area showing the locations of public charging stations

Traffic impacts were quantified using the flow-weighted Travel Time Index (TTI) and total network delay in 30-minute bins from 06:00 to 22:00. Link-level TTI of link ℓ is

$$\text{TTI}_\ell = \frac{T_\ell}{T_\ell^{\text{free}}}. \tag{11}$$

Network-level TTI was the corresponding volume-weighted aggregate across links, and delay was defined as volume-weighted excess travel time above free-flow, aggregated to 30-minute intervals.

3 Results and discussion

Household-level car assignment and driver profiles

The household-level synthetic population closely matches VISTA and report by Ausgrid (2023) in household-type composition (Figure 6). The area-wise EV assignment reproduces the postcode-level EV shares, as shown in Figure 7, confirming that local targets are met while preserving the local household–dwelling composition.

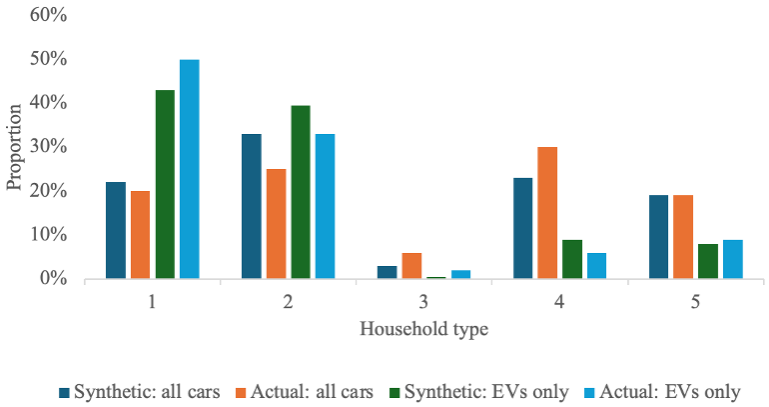


Figure 6: Distribution of household types across synthetic and actual populations

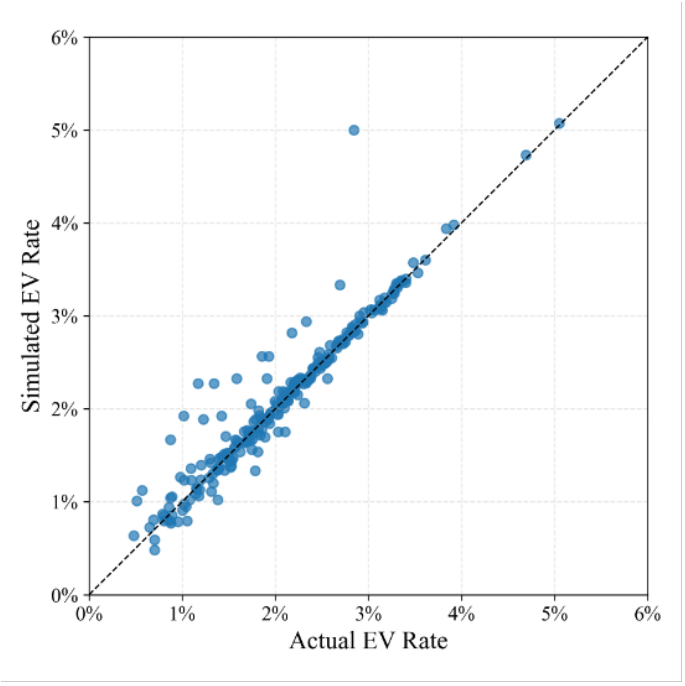


Figure 7: Scatter plot of predicted versus actual electric vehicle allocations by postcode

Household-level car assignment then identifies drivers, and the driver cohort differs across strategies. As shown in Figure 8 and Figure 9, FSFS produces earlier first-trip departures and earlier departure distributions across the first two trips. Figure 10 shows that LDF yields the highest per-driver daily travel distance, while Random produced the lowest.

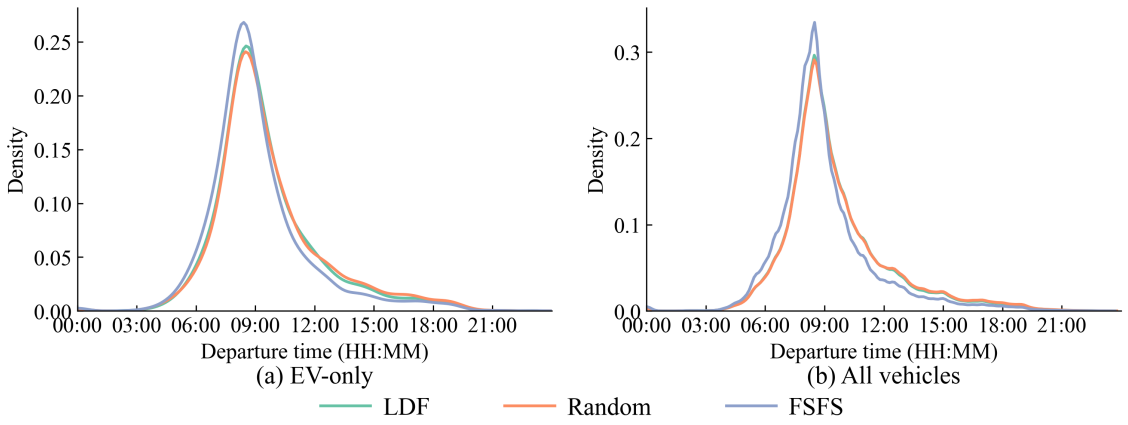


Figure 8: Departure-time distribution of the first trip by drivers under different strategies

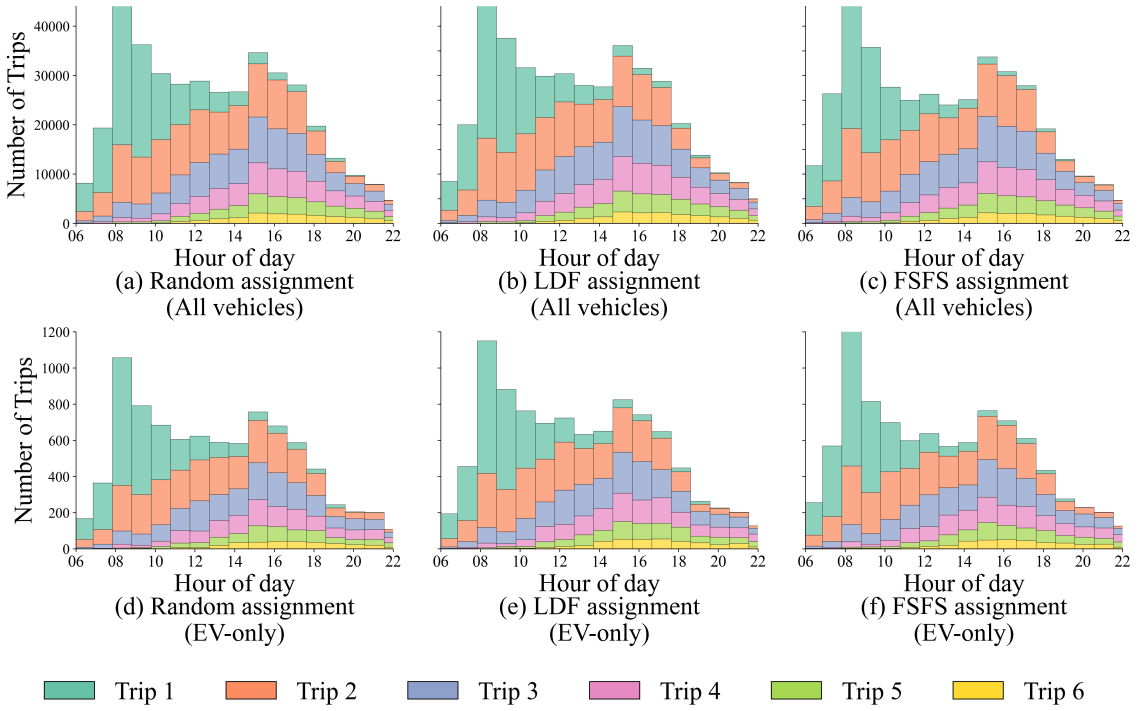


Figure 9: Departure time distribution of first six trips by drivers under different strategies

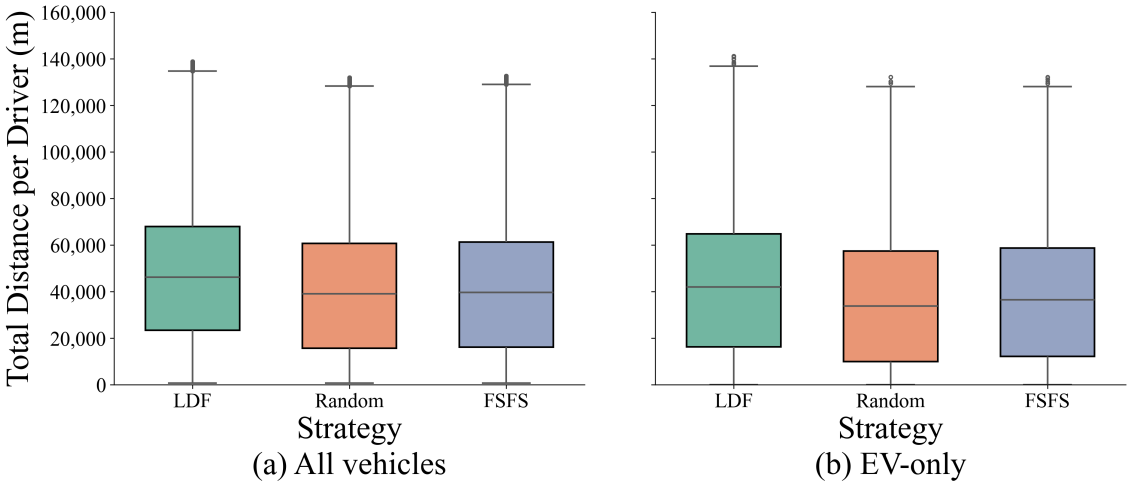


Figure 10: Comparison of per-driver daily travel distance across assignment strategies

Within-household trip assignment outcomes

Within-household trip assignment generated a distinct temporal pattern for pick-up and drop-off events. The processed pick-up/drop-off start times shows clear morning and afternoon peaks (Figure 11), consistent with typical chauffeuring needs. Figure 12 shows an example of within-household car trip assignment. Agent 2093909 is the driver in the household and makes an additional trip (Red) from pick-up to drop-off. The corresponding trips of the passenger agent are changed from "Car" to "Passenger" (Green), which carries no utility in the simulation.

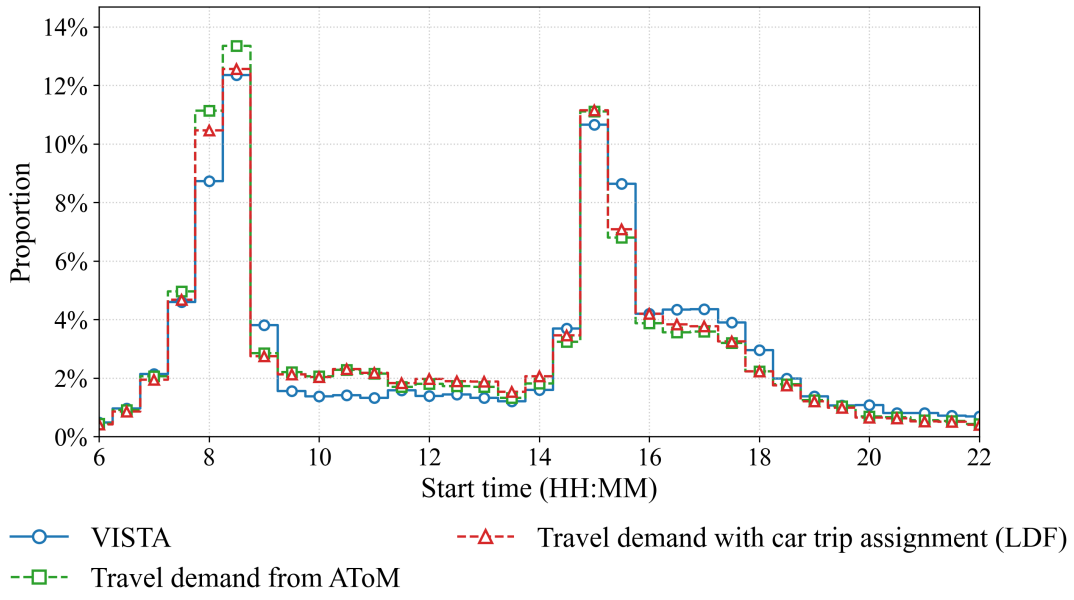


Figure 11: Pick-up and Drop-off Start Time Distribution (30-min bins)

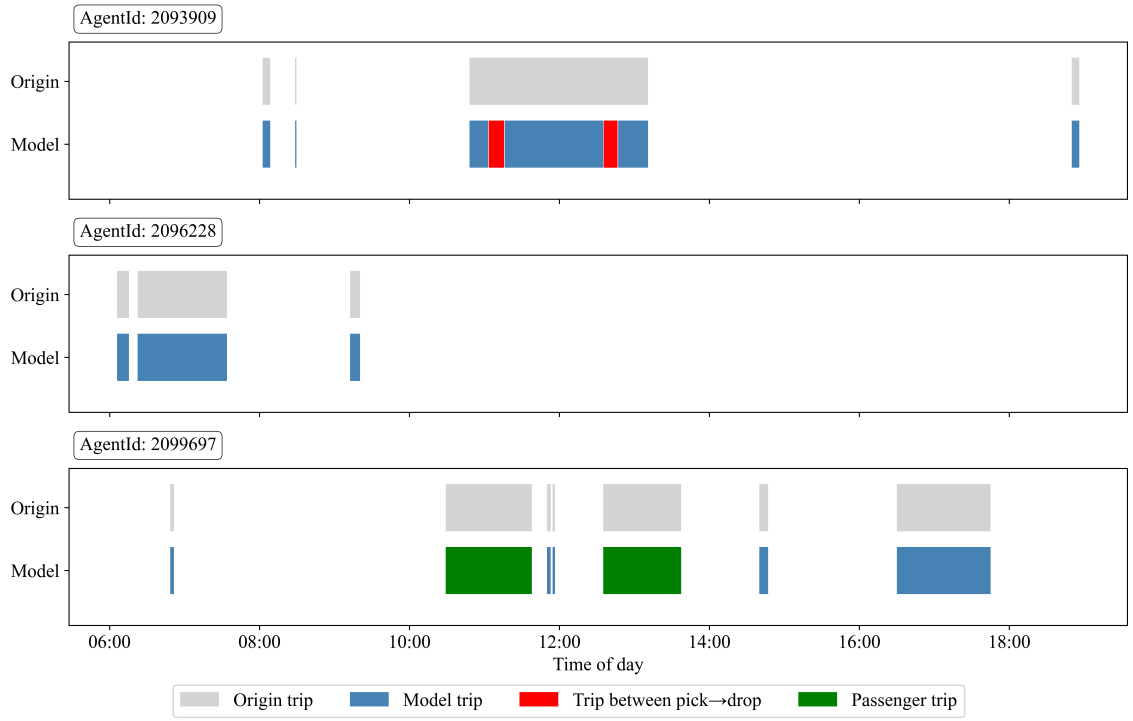


Figure 12: Comparison of agent's trips before and after within-household car trip assignment

Traffic volume and congestion impacts

After household-level car assignment, the temporal profile of en-route vehicles retains the characteristic morning and evening peak structure as shown in Figure 13. However, peak magnitudes are reduced and the ramp-up/ramp-down slopes are smoother (Figure 13a). When normalised, the simulated profile aligns closely with VISTA during the critical peak periods (Figure 13b).

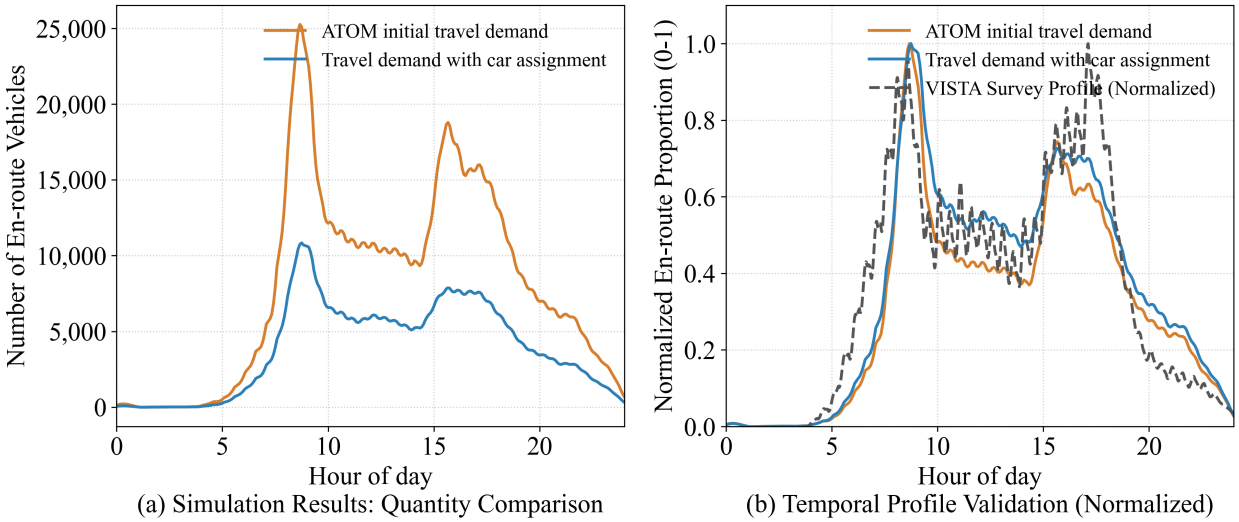


Figure 13: The distribution of en-route vehicles over time

Congestion indicators moves downward correspondingly. The flow-weighted network TTI and total network delay are lower and less volatile over 06:00–22:00 after household-level car assignment (Figures 14a, b), while the timing of peak congestion remains broadly unchanged. As shown in Figure 14c, the share of Vehicle Distance Travelled (VDT) under congestion (TTI $\geq$ 1.10) is similar across the two travel demand profiles and remains broadly stable from 06:00 to 22:00, with a persistent, modest downward shift under household-level car assignment.

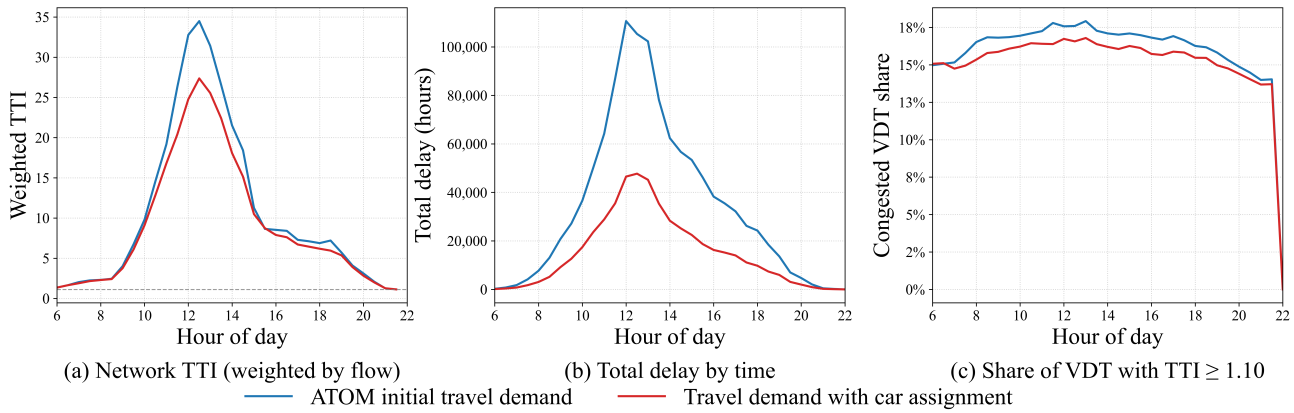


Figure 14: Impact of household-level car assignment on network performance and congestion indicators

Charging outcomes: fleet SoC dynamics

Fleet SoC distributions differs systematically across strategies. As shown in Figure 15, Random maintains a higher share of high-SoC vehicles overnight and in the morning, and a lower share of low-SoC vehicles during the evening peak compared with FSFS and LDF. Mean SoC trajectories corroborates these differences: Random exhibits the highest early-morning mean SoC and a less severe daily minimum, whereas FSFS and LDF reaches lower end-of-day minima (Figure 16).

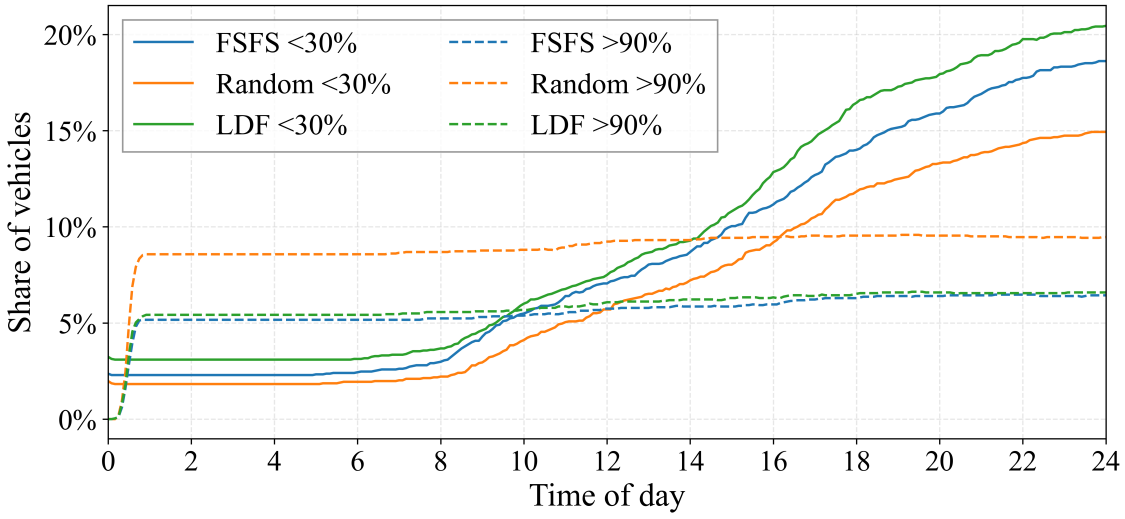


Figure 15: Shares of Low-/High-SOC over time

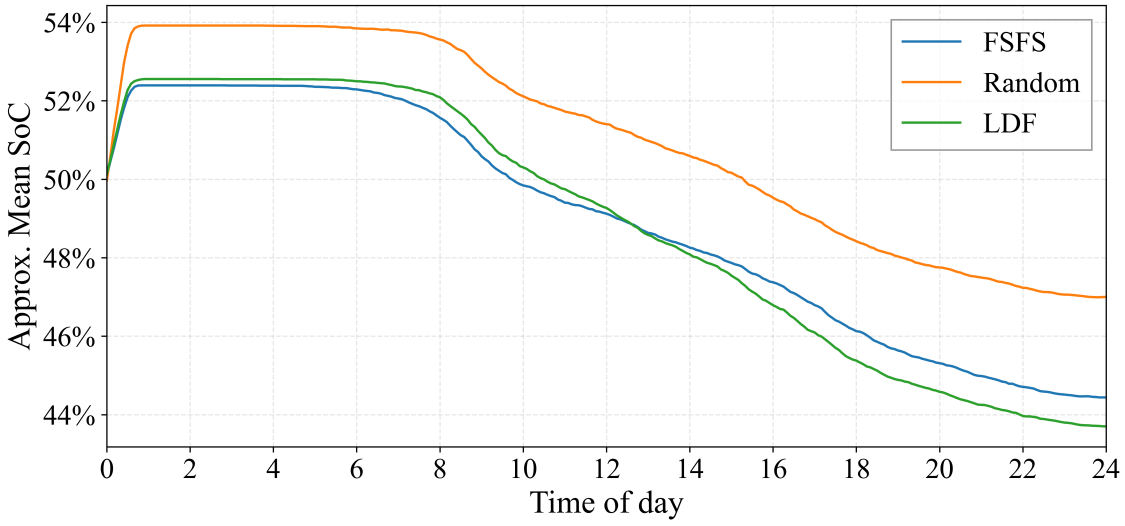


Figure 16: Mean SOC over time

Discussion and implications

Across the case study, household-level car assignment acts as a natural dampener on peak traffic intensity: it reduces peak-hour simultaneity, mitigates the morning peak, and smooths congestion(TTI and delay) without fundamentally shifting the time-of-day pattern. This suggests that approaches assuming unconstrained vehicle access may overestimate peak traffic loads by overlooking negotiated adaptation in household mobility. In addition, within-household trip assignment reduces trip loss and captures the "hidden capacity" of household coordination, preserving mobility under realistic asset limits.

The strategy sensitivity of SoC trajectories has direct implications for charging demand assessment. LDF produces lower average SoC and more deep discharges, consistent with high-utilisation settings such as early adoption or fleet-style prioritisation of EV use. Random maintains a higher overnight buffer and a more distributed SoC profile, which is more representative of a future mass-market context where EV use is embedded in diverse routines. Therefore, charging demand is shaped not only by charging rules and battery technology, but also by how households allocate vehicles; a shift from efficiency-driven to convenience-driven assignment can alter the timing and magnitude of peak grid loads.

Methodologically, the proposed method provides (i) an IPF-based EV-ownership assignment that reproduces postcode penetration while preserving household and dwelling composition, and (ii) a transparent within-household trip assignment that reduces constraint-induced trip loss. The resulting household-level EV demand enables policy analysis focused on mobility constraints and equity (e.g., impacts on secondary drivers in single-EV households).

4 Conclusions

This paper proposed a household-level EV assignment and trip assignment for city-scale agent-based transport simulation, designed to represent private cars as finite, shared household resources rather than assuming unconstrained car access. Using Greater Melbourne as a case study and integrating VISTA, postcode-level EV penetration, and EV-owner household/dwelling marginals, we generated a household-consistent EV-driving population and simulated both traffic and EV energy states under alternative within-household car assignment strategies.

Three main findings emerged. First, enforcing household car availability substantially reduces simultaneous car use and smooths peak traffic intensity while preserving the overall time-of-day structure of travel demand. Second, within-household car trip assignment provides a practical mechanism to reduce constraint-induced trip loss and maintain behavioural plausibility under limited household car resources. Third, EV energy outcomes are highly sensitive to car assignment strategies, implying that charging demand assessments depend not only on charging rules but also on household car assignment.

Overall, the results indicate that household-level interactions are a critical behavioural layer for

realistic EV demand generation and that omitting household resource constraints can bias both congestion and charging demand inferences.

Acknowledgements

Shuai Zhang is supported by a RACE for 2030 Top Up Scholarship as well as RMIT University's RTP scholarship. Afshin Jafari is supported by RMIT University's Vice Chancellor's Research Fellowship program. Chris De Gruyter is supported by an Australian Research Council (ARC) Discovery Early Career Researcher Award (DECRA) (DE220100052).

References

Aemmer, Z., & MacKenzie, D. (2022, 09). Generative population synthesis for joint household and individual characteristics. *Computers, Environment and Urban Systems*, *96*, 101852. doi: 10.1016/j.compenvurbsys.2022.101852

Ausgrid. (2023, 10). *Ev owner demographics and behaviours results of evenergi's relevant surveys.*

Both, A., Singh, D., Jafari, A., Giles-Corti, B., & Gunn, L. (2021, 11). An activity-based model of transport demand for greater melbourne. *arXiv (Cornell University).*

Boulakhbar, M., Farag, M., Benabdelaziz, K., Kousksou, T., & Zazi, M. (2022, 12). A deep learning approach for prediction of electrical vehicle charging stations power demand in regulated electricity markets: The case of morocco. *Cleaner Energy Systems*, *3*, 100039. doi: 10.1016/j.cles.2022.100039

Guo, D., Liu, R., Li, M., Tan, X., Ma, P., & Zhang, H. (2024, 06). An approach to optimizing the layout of charging stations considering differences in user range anxiety. *Sustainable Energy Grids and Networks*, *38*, 101292-101292. doi: 10.1016/j.segan.2024.101292

Horni, A., Nagel, K., & Axhausen, K. W. (2016). *Multi-agent transport simulation matsim.* Ubiquity Press Ltd.

Hu, Y., van Wee, B., & Ettema, D. (2023, 01). Intra-household decisions and the impact of the built environment on activity-travel behavior: A review of the literature. *Journal of Transport Geography*, *106*, 103485. doi: 10.1016/j.jtrangeo.2022.103485

Jafari, A., Singh, D., Both, A., Abdollahyar, M., Gunn, L., Pemberton, S., & Giles-Corti, B. (2024, 07). Activity-based and agent-based transport model of melbourne: an open multi-modal transport simulation model for greater melbourne. *Journal of Intelligent Transportation Systems*, 1-18. Retrieved from `https://arxiv.org/abs/2112.12071` doi: 10.1080/15472450.2024.2372894

Khachman, M., Morency, C., & Ciari, F. (2024, 08). A novel machine learning-based spatialized population synthesis framework. *Transportation*. doi: 10.1007/s11116-024-10534-0

Qiang, Y., Zhou, Y., Gebreyesus, G. D., & Fujimura, S. (2025, 04). Multi-agent trips simulation-based charging demand forecasting. *IEEJ Transactions on Electrical and Electronic Engineering*. doi: 10.1002/tee.70022

Shanmuganathan, J., Victoire, A. A., Balraj, G., & Victoire, A. (2022, 08). Deep learning lstm recurrent neural network model for prediction of electric vehicle charging demand. *Sustainability*, *14*, 10207. doi: 10.3390/su141610207

Wang, S., Zhuge, C., Shao, C., Wang, P., Yang, X., & Wang, S. (2023, 06). Short-term electric vehicle charging demand prediction: A deep learning approach. *Applied Energy*, *340*, 121032. doi: 10.1016/j.apenergy.2023.121032

Weiss, A., & Habib, K. N. (2020, 04). Understanding joint travel and vehicle allocation at the household level through inference of revealed preference data. *Travel Behaviour and Society*, *19*, 207-218. doi: 10.1016/j.tbs.2020.01.006

Wickramasinghe, B. N., Singh, D., & Padgham, L. (2020, 01). Building a large synthetic population from australian census data. *arXiv (Cornell University)*. doi: 10.48550/arxiv.2008.11660

Yang, C., Fu, X., & Dong, R. (2025, 01). Investigating spatial-temporal characteristics of joint activity/travel behaviour with smart card data. *Travel Behaviour and Society*, *38*, 100899. doi: 10.1016/j.tbs.2024.100899

Zhang, Y., Xu, S., Xu, J., Zeng, X., Li, Z., & Xie, C. (2023, 02). Robust charging demand prediction and charging network planning for heterogeneous behavior of electric vehicles. *Journal of Shanghai Jiaotong University (Science)*, *28*, 136-149. doi: 10.1007/s12204-023-2576-0